Second sound in SrTi03

Second Sound in $SrTiO_3$

Akitoshi Koreeda, Ryuta Takano, and Seishiro Saikan

Department of Physics, Graduate School of Science, Tohoku University, Sendai 980-8578, Japan

(Received 6 August 2007; published 28 December 2007)

We study collective phonon excitations in $SrTiO_3$ by low-frequency light scattering. We employ extended thermodynamics for phonon gas to construct a theoretical spectral function that is applicable regardless of local thermal equilibrium. Our analysis reveals the temperature dependence of τ_N, the relaxation time for the momentum-conserving phonon collisions (normal processes), in $SrTiO_3$. These results indicate that the previously reported anomalous soundlike spectrum originates from second sound, which is a wavelike propagation of heat.

DOI: 10.1103/PhysRevLett.99.265502 PACS numbers: 63.20.−e, 05.70.Ln, 66.70.+f, 77.84.Dy

$SrTiO_3$ and $KTaO_3$ have provided many interesting phenomena that may be attributable to the large anharmonicity and large zero-point motion in these materials, which are called ''quantum paraelectrics'' [1]. In such highly anharmonic systems, collective phonon excitation plays an important role in energy transport, where thermal diffusion, the ''second-sound'', or the kink-soliton wave are thought to occur, based on molecular dynamics simulations [2]. Second sound is a wavelike propagation of entropy or temperature [3], and it must be studied carefully because ''temperature'' should effectively modulate or couple with many other elementary excitations. In solids, however, second sound is rarely observed or investigated, except in solid He, isotopically clean samples of NaF, and Bi [4,5]; this is because it simultaneously requires both sufficiently rare resistive (momentum-destroying) phonon-phonon collisions (including umklapp and impurity scattering processes) and sufficiently frequent normal (momentum-conserving) ones [6]. Furthermore, the expected second-sound frequency is too low for second sound to be observed in most dielectrics in large-angle light-scattering experiments with visible light sources [5]. However, it has been proposed theoretically [7] that second sound may exist in $SrTiO_3$ because the normal phonon collision should be rather frequent due to strong interaction between long-wavelength, ''soft'' (low-frequency) optical phonons, and acoustic phonons [8]. The second-sound frequency in such a system should be in the 10 GHz range, which is observable in ordinary light-scattering experiments. More recently, an anomalous soundlike spectrum has been observed in a Brillouin light-scattering experiment in $SrTiO_3$, and this spectrum has been tentatively ascribed to second sound [9]. If second sound with such a high frequency exists, a coherent or large-amplitude excitation of this ''entropy wave'' might be realized by optical methods [10], and this wave, in turn, should enable us to drastically modulate various excitations in $SrTiO_3$ and related materials. However, since little information is available on the normal collision rate, the existence of second sound in $SrTiO_3$ is still controversial, as a number of negative reports have been published by other authors [11].

In this Letter, we present a theoretical background that helps us understand the experimental spectra from the gas of phonons, and we analyze the experimental data to obtain important and novel phonon-gas characteristics, namely, the temperature dependences of τ_N and τ_R, which are the relaxation times for normal and resistive phonon-collision processes, respectively. Fits of the newly obtained theoretical expression to the experimental light-scattering spectra strongly suggest that the origin of the anomalous doublet-spectrum is second sound.

Recently, a nonequilibrium phenomenology called extended (-irreversible) thermodynamics (ET) has been recognized as a powerful means of describing many nonequilibrium aspects of transport phenomena [12]. From the one-dimensional ET equation of a mixture of longitudinal and transverse acoustic (LA and TA) phonons [13], we have recently derived an expression for the scattering spectrum due to energy fluctuations in phonon gas [14]. The result for LA phonon gas in the Fourier-Laplace space is

$$S_{\mathrm{ET}}^{\mathrm{LA}}(q,s)=\frac{\gamma_1^{(l)}[1-\frac{2}{9\tau_N^2}(s+\frac{a^{(t)}}{3\tau})\gamma_2^{(l)}(\gamma_1^{(t)}\gamma_2^{(t)})]}{1-\frac{2}{9\tau^2}\gamma_1^{(l)}\gamma_1^{(t)}-\frac{2\omega_0^2}{27\tau_N^2}W^{(l)}(s)(\gamma_1^{(l)}\gamma_2^{(l)})(\gamma_1^{(t)}\gamma_2^{(t)})}, \tag{1}$$

where we have assumed for simplicity an average group velocity of phonons $\bar{c}$ and average relaxation times τ_N and τ_R for both LA and TA modes, and we have defined that $\tau^{-1}=\tau_N^{-1}+\tau_R^{-1}$. In Eq. (1), the natural frequency of a phonon gas is defined as

$$\omega_0 \equiv \bar{c}q/\sqrt{3}, \tag{2}$$

with the scattering wave-vector magnitude $q=2k\sin(\theta/2)$, where k is the wave-vector magnitude of the incident probe (such as that of light) and θ is the scattering angle. The spectrum for TA mode, $S_{\mathrm{ET}}^{\mathrm{TA}}(q,s)$, is given simply by interchanging the superscripts: $(l)\rightarrow(t)$, and vice versa. The total spectrum is a linear combination of $S_{\mathrm{ET}}^{\mathrm{LA}}(q,s)$ and $S_{\mathrm{ET}}^{\mathrm{TA}}(q,s)$, viz.,

$$S_{\mathrm{ET}}(q,\omega)=\mathrm{Re}[p_1 S_{\mathrm{ET}}^{\mathrm{LA}}(q,s)+p_2 S_{\mathrm{ET}}^{\mathrm{TA}}(q,s)]_{s=i\omega}, \tag{3}$$

where p_1 and p_2 are weighting coefficients. In Eq. (1), $\gamma^{(\lambda)}$s are continued-fraction expressions for the spectrum for LA and TA phonon gases, respectively, where λ represents the phonon mode either LA (l) or TA (t). $\gamma^{(\lambda)}$s are recursively given as $\gamma_m^{(\lambda)} = [s + \tau^{-1} + \alpha_{m+1}\bar{c}^2q^2\gamma_{m+1}^{(\lambda)}]^{-1} (m \geq 3)$, with $\gamma_2^{(\lambda)} = [s + \tau_R^{-1} + \alpha_2 a^{(\lambda)}\tau_N^{-1} + \alpha_3\bar{c}^2q^2\gamma_3^{(\lambda)}]^{-1}$, $\gamma_1^{(\lambda)} = [s + \alpha_2 a^{(\lambda)}\tau^{-1} + \alpha_2\bar{c}^2q^2\gamma_2^{(\lambda)}]^{-1}$, where $a^{(\lambda)} = 2, 1$ for $(\lambda) = (l), (t)$, respectively, and α_m is defined as $\alpha_m \equiv (m-1)/[4(m-1)^2 - 1](m \geq 2)$ [13]. Finally, $W^{(l)}(s)$ is given as $W^{(l)}(s) = 2\tau_N\tau^{-1}[1 + 4\gamma_1^{(l)}\gamma_2^{(l)}/(9\tau_N\tau)] - \omega_0^{-2}(s + a^{(l)}/3\tau) \times (s + a^{(t)}/3\tau - a^{(t)}\gamma_1^{(l)}/9\tau^2)$ and $W^{(t)}(s)$ is given by letting $(l) \rightarrow (t)$, and vice versa, in $W^{(l)}(s)$. Although this phenomenological formalism appears to deal with only the LA-TA coupling, it can be understood that the relaxation processes of each mode toward the equilibrium distributions should effectively involve interactions with other excitations, such as optic phonons or impurities [13].

Since Eq. (3) is too complicated to capture the physical significance of the spectral components, we need a simpler expression with appropriate approximations. If phonon collisions take place frequently enough within the observation-length scale, i.e., either $\bar{c}\tau_N \ll q^{-1}$ or $\bar{c}\tau_R \ll q^{-1}$ holds ("hydrodynamic regime"), Eq. (3) can be well approximated as the sum of two spectra: one arises from a damped harmonic oscillator (DHO) of a collective, thermalized phonon gas and the other arises from kinetic collisions between individual phonons. Thus, for the hydrodynamic regime, we have

$$S_{\mathrm{HD}}(q,\omega) \approx P_1 \frac{2\omega_0^2\Gamma_{\mathrm{ss}}}{(\omega^2-\omega_0^2)^2 + 4\omega^2\Gamma_{\mathrm{ss}}^2} + P_2\frac{\Gamma_2}{\omega^2+\Gamma_2^2}, \quad (4)$$

where we have defined Γ_{ss} and Γ_2 as

$$\Gamma_{\mathrm{ss}} \equiv (2/15)\bar{c}^2q^2\tau_N + (2\tau_R)^{-1}, \quad (5a)$$

$$\Gamma_2 \equiv \tau_N^{-1} + \tau_R^{-1} + 1.23\bar{c}q, \quad (5b)$$

where P_1 and P_2 are weighting coefficients, which depend on the strength of the coupling between phonon modes. It is an important new feature that the "thermodynamic" DHO spectrum is superposed on a broader nonthermodynamic central peak.

If $\Gamma_{\mathrm{ss}} \gg \omega_0$, the DHO is heavily overdamped. The first term in Eq. (4) can then be further approximated as a central Lorentzian due to thermal diffusion, whose width is given by $\Gamma_1 \approx D_{\mathrm{th}}q^2 \ll \Gamma_2$, where $D_{\mathrm{th}} \equiv \frac{1}{3}\bar{c}^2\tau_R$ is the thermal diffusivity. In this case, $S_{\mathrm{HD}}(q,\omega)$ should consist of two unshifted Lorentzians. This phenomenon has been actually observed in many dielectric crystals, including $SrTiO_3$ [15,16], but the origin of the broader Lorentzian has been unknown in the 30 years since its first report [15]. The observed linewidth for the broader Lorentzian had little dependence on q, and it was approximately proportional to T [15,16]. These features can be explained in terms of Eq. (5b) with the fact that the phonon-collision rate τ^{-1} is proportional to the number of thermally excited phonons. It is worth noting that the two-phonon difference light-scattering mechanism, which was previously proposed as the origin for the broader central peak [15], can be shown to be a special case in the ET description of light scattering [14].

If $\Gamma_{\mathrm{ss}} < \omega_0$, the DHO is underdamped and exhibits a resonance at a frequency

$$\omega_{\mathrm{ss}} = \sqrt{\omega_0^2 - \Gamma_{\mathrm{ss}}^2} \approx \frac{1}{\sqrt{3}}\bar{c}q\left(1 - \frac{2}{5}\frac{\tau_N}{\tau_R}\right). \quad (6)$$

This is the "second-sound" resonance [2], and entropy now "propagates" at a velocity slightly slower than $\bar{c}/\sqrt{3}$. Equation (4) shows that the second-sound spectrum must be generally accompanied by a broader central Lorentzian with a width of Γ_2. Note also that the widths of the broad central Lorentzian and that of the second-sound doublet are not independent: both linewidths are essentially determined by four common parameters, τ_N, τ_R, $\bar{c}$, and q.

We measured the temperature dependence of the low-frequency light-scattering spectra in $SrTiO_3$ in the temperature range of 295 to 6.4 K with $\boldsymbol{q}$-vector ($|\boldsymbol{q}| = 6.0 \times 10^7$ m^{-1}) set parallel to the crystalline [100] direction in the high-T cubic symmetry [16]. The recorded spectra are reproduced in Fig. 1 at a higher resolution than in Ref. [16]. It is clearly seen that, for relatively high temperatures, the spectra consist of two Lorentzians centered at $\omega = 0$. As the temperature decreases, the narrower component broadens while the broader one narrows [16]. This can be explained from the expressions for Γ_1 and Γ_2. Although the crystal was not oriented under 105 K, at which $SrTiO_3$ undergoes a structural phase transition from cubic to

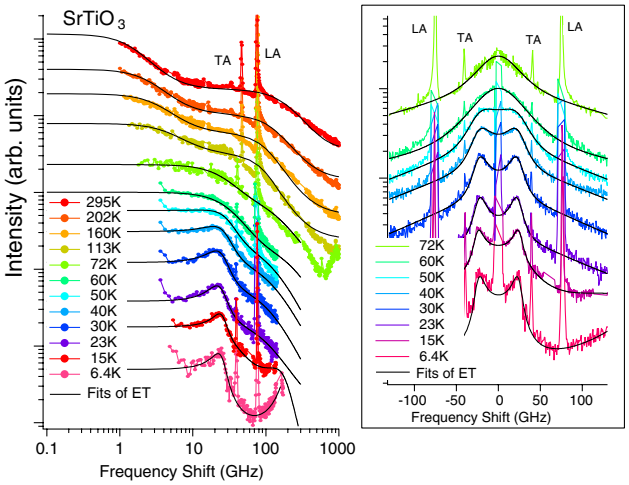

FIG. 1 (color online). Temperature dependence of the low-frequency light-scattering spectra in $SrTiO_3$ from 6 to 295 K (log-log plot). "LA" and "TA" denote longitudinal and transverse acoustic phonons' Brillouin lines, respectively. The inset is a semilog plot for the spectra below 72 K. Each spectrum is appropriately scaled for visual clarity. The solid lines are fits of Eq. (3).

tetragonal symmetry, our sample exhibited a clear doublet spectrum superposed on a broad central Lorentzian. As reported [9,17], the observed broad doublet had a characteristic of soundlike excitation; i.e., the frequency shift was linearly proportional to q. In addition, the observed linewidth of the broad doublet has been reported to vary as q^p, where p is a constant close to but smaller than 2 [17]. These two aspects for the shift and the linewidth are in good agreement with Eqs. (6) and (5a), respectively.

In fitting the formula Eq. (3) or Eq. (4), we set the value for τ_R as a known parameter, estimated from the relation $\tau_R = 3D_{\rm th}/v_D^2$, where $v_D \approx 5400$ m/s is the averaged sound velocity generally employed in Debye's model [3]. The temperature dependence of $D_{\rm th}$ was measured separately [16] by the impulsive stimulated thermal scattering technique [10]. The values of $D_{\rm th}$ so obtained were already confirmed to be consistent with the published values [16]. Thus, five parameters were adjusted in the fitting: for Eq. (3), τ_N, $\bar{c}$, p_1, p_2, and $C_{\rm bg}$; for Eq. (4), τ_N, $\bar{c}$, P_1, P_1, and $C_{\rm bg}$, where $C_{\rm bg}$ is a constant background. We could better fit the spectra observed at 6.4 and 15 K if we replaced the constant background with an appropriate inelastic structure [9] arising from first-order Raman scattering by a softened transverse optic phonon mode [18]. The observed spectra have been quite well fitted by both Eqs. (3) and (4) in the temperature range below 100 K. At higher temperatures, the experimental spectra were better fitted if we distinguished the sound velocities and the relaxation times for LA and TA modes in the ET expression instead of regarding them as common ones. Below 100 K, the reproduced spectra for the two expressions in Eqs. (3) and (4) almost indistinguishably coincided with each other above ~20 K, although only slightly different values for τ_N were obtained. Below 20 K, however, systematic deviations between the two models occurred, and the obtained values for τ_N were significantly different at 6.4 K.

Figure 2 shows the temperature dependence of τ_N^{-1} obtained in the present analysis and that of τ_R^{-1} obtained in the previous work [16]. Below ~50 K, τ_N^{-1} gradually deviates from τ_R^{-1}, seemingly giving rise to a frequency window for second-sound observation (the region between the lines for τ_N^{-1} and τ_R^{-1} in Fig. 2). The fact that the fitted τ_N, $\bar{c}$, and the known τ_R simultaneously satisfy Eqs. (2) and (5) implies the high reliability of our analysis. In fact, the values obtained for $\bar{c}$ ranged from 3600 m/s at 6.4 K to 5900 m/s at 50 K, which are quite reasonable compared with $v_D = 5400$ m/s. The value of τ_N can be roughly evaluated from the Gurevich-Tagantsev relation [7], $\tau_U/\tau_N \sim \chi^{1/2}$, where τ_U and χ are the umklapp scattering time and the dielectric constant, respectively. Replacing τ_U with τ_R, which is smaller than τ_U in general, and substituting the known value for χ (~10^{3-4} for $T \sim 20$ K [19]), τ_N^{-1} is expected to be on the order of 10^{12} rad/s or less for $T \sim 20$ K; this does not contradict our result.

We also show in Fig. 2, the second-sound frequency, $\omega_{\rm ss}$, and the linewidth, $\Gamma_{\rm ss}$, estimated, respectively, from

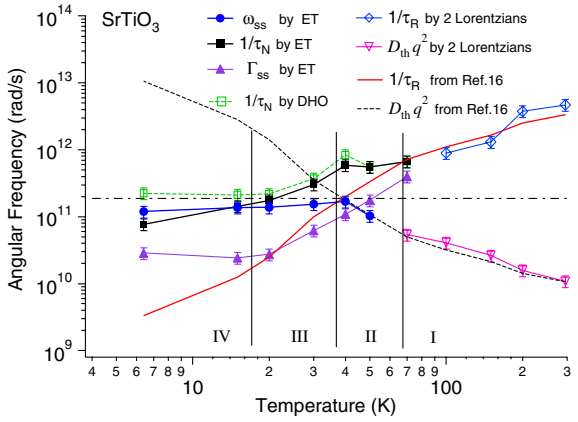

FIG. 2 (color online). Temperature dependences of the normal (τ_N^{-1}) and resistive (τ_R^{-1}) phonon relaxation rates. Legend is shown in the figure. The temperature regions are labeled I, II, III, and IV according to the definition in the text. The second-sound regime corresponds to region III. All the lines between the symbols are guides for the eye. The dashed horizontal line at $\sim 2 \times 10^{11}$ rad/s represents a constant $qv_D/\sqrt{3} \approx \omega_0$.

Eqs. (6) and (5). It is seen that several temperature ranges may be defined according to the relation between $\omega_{\rm ss}$, τ_N^{-1} and τ_R^{-1}: (I), $T > 70$ K; (II), $40 \lesssim T \lesssim 70$ K; (III), $20 \lesssim T \lesssim 40$ K; (IV), $T \lesssim 20$ K. Region I ($T > 70$ K) corresponds to the case of heavily damped second sound, i.e., thermal diffusion regime, and the observed spectra consist of two unshifted Lorentzians as we have shown in Fig. 1. The fitting result was not sensitive to the value of τ_N in this temperature range, and no value for τ_N^{-1} is shown. The values obtained by fitting Eq. (3) with different values of c and τ for the LA and TA modes to the observed spectra yielded reasonable values of $\tau_R^{(l)}$ and $\tau_R^{(t)}$ [20], for which an averaged value for τ_R was calculated as $\tau_R^{-1} = 1/\tau_R^{(l)} + 1/\tau_R^{(t)}$. $\Gamma_1 = D_{\rm th}q^2$ was reproduced from the relation $D_{\rm th} = \frac{1}{3}v_D^2 q^2 \tau_R$. In Fig. 2, τ_R^{-1} and Γ_1 so obtained are plotted as $\diamond$ and $\triangledown$, respectively; these values are in good agreement with the known values. In region II ($40 \lesssim T \lesssim 70$ K), the second-sound window begins to open up slightly, but the second sound is still overdamped (or nearly critically damped) because $\omega_0 \lesssim \Gamma_{\rm ss}$, resulting in the round, non-Lorentzian, quasielastic peak shown in Fig. 1. In region III ($20 \lesssim T \lesssim 40$ K), we see that $\tau_R^{-1} < \omega_{\rm ss} < \tau_N^{-1}$, and we are now in the second-sound regime although the window condition is not as genuine as the classical one, viz., $\tau_R^{-1} \ll \omega_{\rm ss} \ll \tau_N^{-1}$ [6]. In region IV ($T \lesssim 20$ K), we see that τ_N^{-1} tends to become slower than $\omega_{\rm ss}$. This means that local thermal equilibrium cannot be established within the relevant scales of space and time. In this temperature range (IV), therefore, the macroscopic expression Eq. (4) is not valid, providing the seemingly incorrect values of τ_N^{-1} obtained by the fit of Eq. (4) for the low temperatures, namely, 6.4 K and 16 K (shown by $\square$ in Fig. 2). In contrast, the ET-fitted τ_N^{-1} easily cuts across $\omega_{\rm ss}$ at around 16 K, and τ_N^{-1} becomes even less frequent than $\omega_{\rm ss}$ at 6.4 K. This

indicates that ET is applicable even when local thermal equilibrium is violated [12]. Accordingly, the broad doublet cannot be ascribed to second sound in its strict sense. This is, however, just an issue of observation, and second sound itself should exist down to even lower temperatures because the frequency window seems to be open for temperatures below 6.4 K. Since it can be shown that the ET spectrum asymptotically becomes equivalent to the two-phonon difference spectrum as τ_R, $\tau_N \rightarrow \infty$ [14], the spectrum in this nonequilibrium regime may be roughly stated as arising due to two-phonon difference light-scattering.

Next, we discuss the reported directional dependence of the quality of the broad-doublet spectrum [9,21]. This anisotropy of the broad doublet has also been a point of controversy, because isotropic second sound cannot explain such anisotropy. In our opinion, however, it can be interpreted simply in terms of elastic anisotropy. In fact, we see that Γ_{ss} in Eq. (5a) contains a quadratic dependence on $\bar{c}$, which depends strongly on the crystalline direction. τ_N and τ_R also exhibit strong directional dependence, leading to an effective anisotropy in phonon density. The present one-dimensional ET analysis can be applied for $\boldsymbol{q}$ in any crystalline direction with appropriate values for $\bar{c}$, τ_N, and τ_R for the relevant direction. As can be expected from Fig. 2, different combinations of $\bar{c}$, τ_N, and τ_R can change the size and position of the second-sound window relative to the frequency ω_{ss}, leading to a change in the quality factor of second-sound resonance, or even to the violation of local thermal equilibrium, depending on the crystalline direction.

Finally, we discuss the absorption length of the observed excitation and a possibility of a localized second sound in small regions. A length $\alpha_{ss}^{-1} \equiv v_{ss}/\Gamma_{ss}$, where $v_{ss} = \omega_{ss}/q$ is the velocity of the second sound, corresponds to the distance at which the intensity of the second sound decreases to $1/e$. For our results in temperature region III, α_{ss}^{-1}s were estimated to be 30, 45, and 85 nm at 40, 30, and 20 K, respectively. These values are only several times larger than the reported sizes for the ferroelectric microregion (FMR) in $SrTiO_3$ [22], and the temperature dependence of α_{ss}^{-1} is reminiscent of that of FMR [22]. Thus, it may be considered that the second sound in $SrTiO_3$ is localized around FMRs, which should contain sufficient numbers of normal phonons [7].

In summary, we have derived the expression for a light-scattering spectrum in interacting phonon gas from the ET equations of Dreyer and Struchtrup [13]. We have successfully fitted the spectral expression to the experimental spectrum from 295 to 6.4 K in $SrTiO_3$ in a unified manner, and we have revealed the temperature dependence of τ_N in $SrTiO_3$. From the measured values of τ_N and τ_R, we have shown that a frequency window for the observation of second sound gradually opens up below ~40 K. Finally, we have concluded that the broad doublet spectrum at around 30 K arises from second sound. Below 20 K, second sound in a classical sense, i.e., as a ''wave of entropy'', cannot be defined well for the employed value of q because entropy is not defined locally for the observation scales of space and time.

This research was partially supported by a Grant-in-Aid for Young Scientists B (for A. K.), 18740171, 2007, from the Ministry of Education, Science, Sports, and Culture of Japan.

[1] E. Courtens, B. Hehlen, G. Coddens, and B. Hennion, Physica (Amsterdam) **219–220B**, 577 (1996), and see references therein.
[2] T. Schneider and E. Stoll, Phys. Rev. B **17**, 1302 (1978); Phys. Rev. B **18**, 6468 (1978).
[3] C. Kittel, *Quantum Theory of Solids* (Wiley, New York, 1963).
[4] C. C. Ackerman, B. Bertman, H. A. Fairbank, and R. A. Guyer, Phys. Rev. Lett. **16**, 789 (1966); H. E. Jackson, C. T. Walker, and T. F. McNelly, Phys. Rev. Lett. **25**, 26 (1970); V. Narayanamurti and R. C. Dynes, Phys. Rev. Lett. **28**, 1461 (1972).
[5] D. W. Pohl and V. Irniger, Phys. Rev. Lett. **36**, 480 (1976).
[6] R. A. Guyer and J. A. Krumhansl, Phys. Rev. **148**, 778 (1966).
[7] V. L. Gurevich and A. K. Tagantsev, Zh. Eksp. Teor. Fiz. **94**, 370 (1988) [Sov. Phys. JETP **67**, 206 (1988)].
[8] J. D. Axe, J. Harada, and G. Shirane, Phys. Rev. B **1**, 1227 (1970); A. Bussmann-Holder, Phys. Rev. B **56**, 10 762 (1997).
[9] B. Hehlen, A.-L. Pérou, E. Courtens, and R. Vacher, Phys. Rev. Lett. **75**, 2416 (1995).
[10] K. A. Nelson, R. J. D. Miller, D. R. Lutz, and M. D. Fayer, J. Appl. Phys. **53**, 1144 (1982).
[11] J. F. Scott, A. Chen, and H. Ledbetter, J. Phys. Chem. Solids **61**, 185 (2000); M. Yamaguchi, T. Yagi, Y. Tsujimi, H. Hasebe, R. Wang, and M. Itoh, Phys. Rev. B **65**, 172102 (2002).
[12] D. Jou, J. Casas-Vázquez, and G. Lebon, *Extended Irreversible Thermodynamics* (Springer, Berlin, 2001), 3rd ed.; I. Müller and T. Ruggeri, *Rational Extended Thermodynamics* (Springer, Berlin, 1998), 2nd ed.
[13] W. Dreyer and H. Struchtrup, Continuum Mech. Thermodyn. **5**, 3 (1993).
[14] A. Koreeda, R. Takano, and S. Saikan (to be published).
[15] K. B. Lyons and P. A. Fleury, Phys. Rev. Lett. **37**, 161 (1976).
[16] A. Koreeda, T. Nagano, S. Ohno, and S. Saikan, Phys. Rev. B **73**, 024303 (2006).
[17] Y. Tsujimi and H. Uwe (unpublished).
[18] J. M. Worlock and P. A. Fleury, Phys. Rev. Lett. **19**, 1176 (1967).
[19] K. A. Müller and H. Burkard, Phys. Rev. B **19**, 3593 (1979).
[20] $c^{(l)}$ and $c^{(t)}$ were fixed to 8021 m/s and 4921 m/s, which were measured from the Brillouin shifts.
[21] E. Farhi, A. K. Tagantsev, B. Hehlen, R. Currat, L. A. Boatner, and E. Courtens, Physica (Amsterdam) **276B**, 274 (2000).
[22] H. Taniguchi, M. Takesada, M. Itoh, and T. Yagi, J. Phys. Soc. Jpn. **73**, 3262 (2004).